Detection of Emerging Sunspot Regions in the Solar Interior

Stathis Ilonidis, Junwei Zhao, and Alexander Kosovichev

Stanford University

LoHCo Workshop
August 17-19, 2011
Stanford, CA

Emerging Magnetic Flux

Goals:

1. To detect the Emerging Magnetic Flux before the start of magnetic field emergence in the photosphere.
2. To predict the evolution of an emerging flux region soon after the start of magnetic field emergence in the photosphere.

Scientific Benefit:

1. Depth of generation of magnetic active regions
2. Strength of magnetic field deep inside the convection zone
3. Structure and kinematics of emerging flux in the convection zone
4. Speed of emerging flux
5. Formation of sunspots and active regions

Practical Benefit:

1. Space weather forecast

Method (part I)

1. We select an annulus on the surface and we uniformly divide it into 6, 8, 10, 12, and 14 arcs.
2. The oscillation signal is averaged inside the arc.
3. Cross-covariances are computed between diametrically opposite arcs (same color).

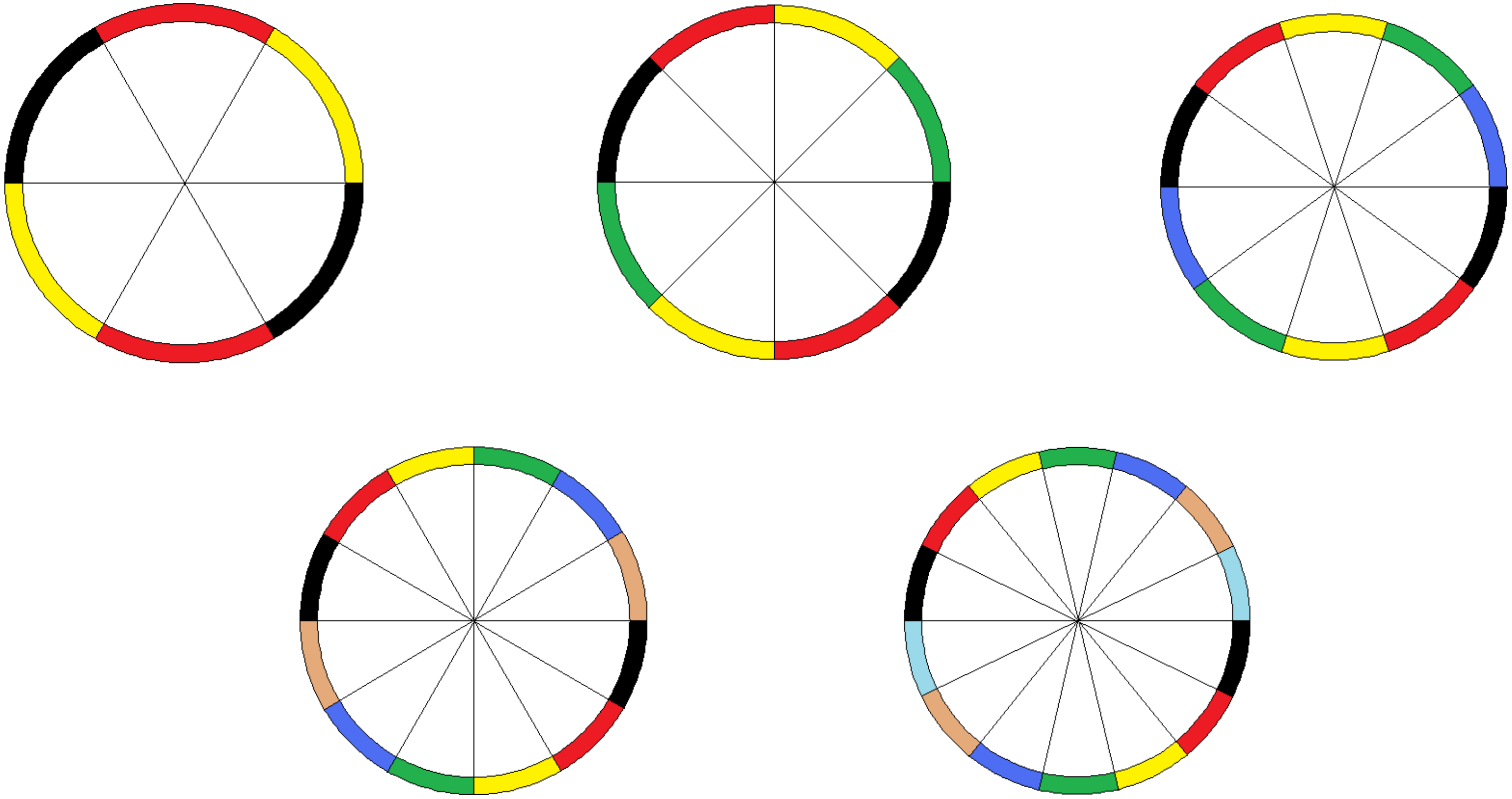

Method (part II)

4. We use 4 orientations for each of the five arc lengths (20 configurations in total).

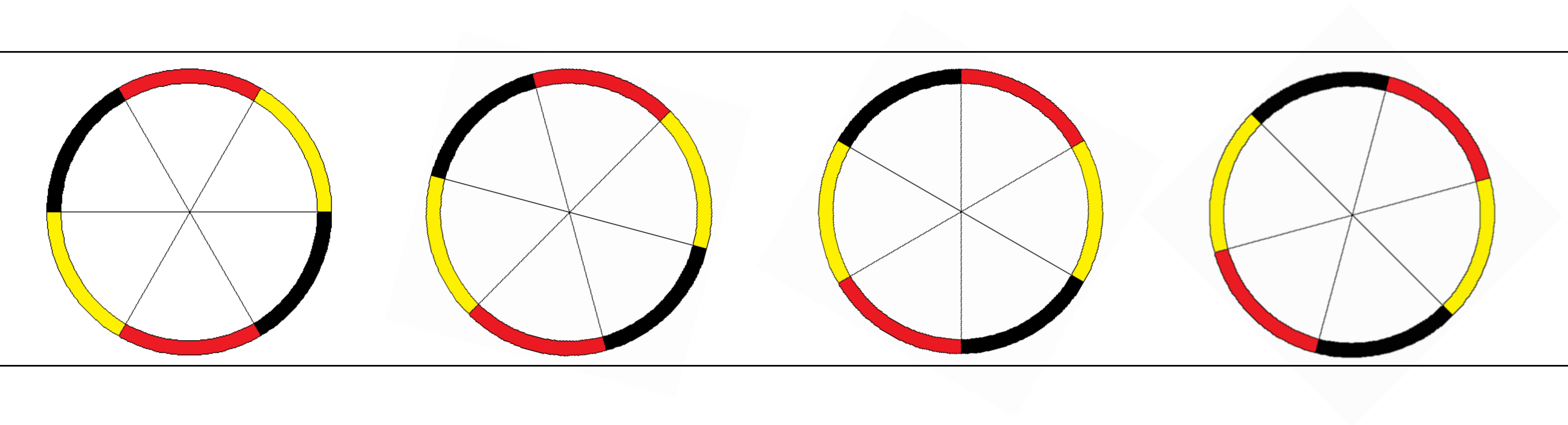

5. All of the cross-covariances are added together to increase the signal-to-noise ratio.
6. Steps 1 - 5 are repeated for 31 annuli. All of the cross-covariances are added together to further increase the signal-to-noise ratio.
7. The final cross-covariance is fitted with a Gabor wavelet and the acoustic phase travel time is obtained.

Data

Tracking & Remapping:

▪ Data:	MDI/HMI Dopplergrams
▪ Tracking rate:	Carrington
▪ Remapping:	Postel’s projection
▪ Duration:	8 hours
▪ Size:	256 X 256 pixels
▪ Spatial Resolution:	0.12 degrees/pixel
▪ Temporal Resolution:	1 minute/45 s

Processing:

▪ Frequency filter:	2 – 5 mHz
▪ Phase-speed filter:	92 – 127 km/s

Acoustic Waves

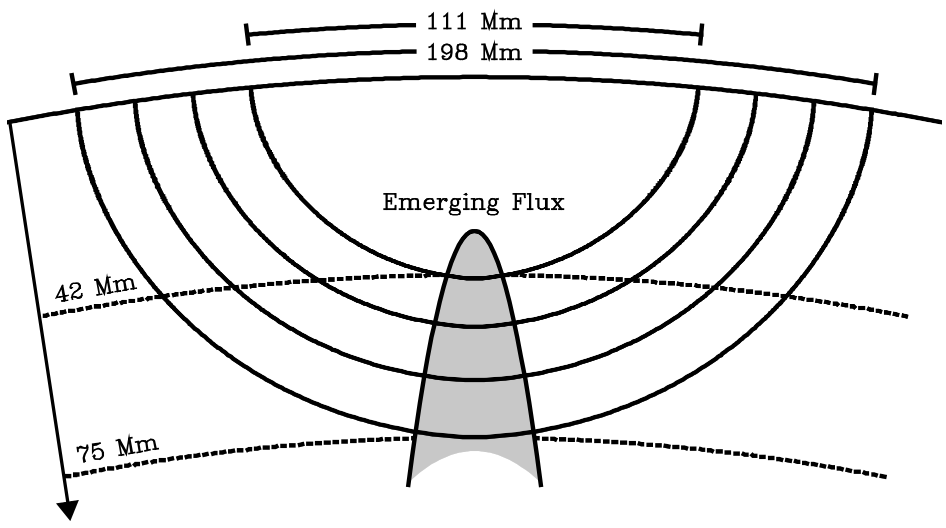

Depth Range: 42 – 75 Mm

1-skip Horizontal Distance: 111 – 198 Mm

Results

- Travel-time maps of 5 emerging flux regions:
  1. AR NOAA 10488 (MDI)
  2. AR NOAA 8164 (MDI)
  3. AR NOAA 8171 (MDI)
  4. AR NOAA 7978 (MDI)
  5. AR NOAA 11158 (HMI)

- Travel-time maps of 9 quiet regions → Estimate of noise level

Results of AR 10488

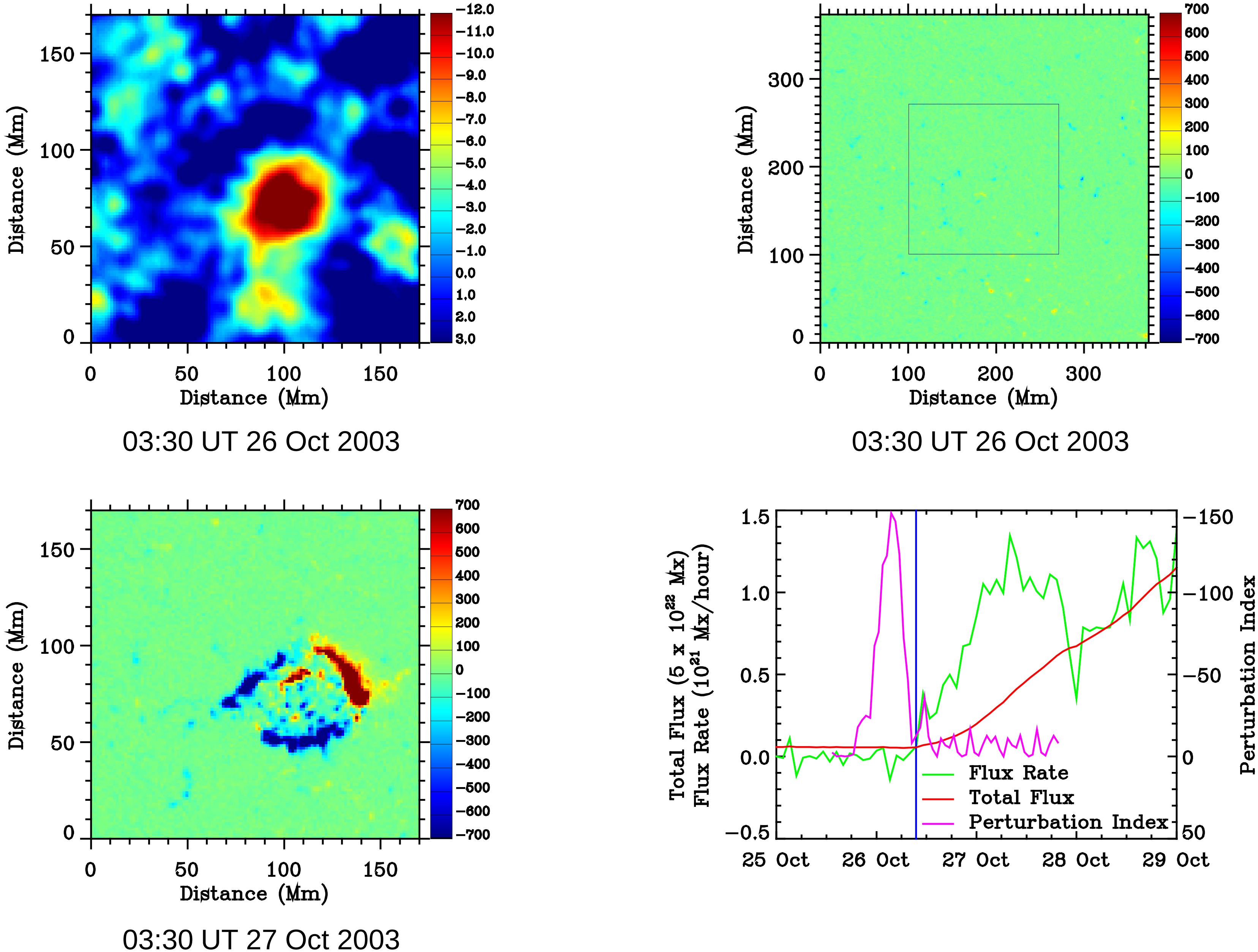

Travel-time maps of AR 10488

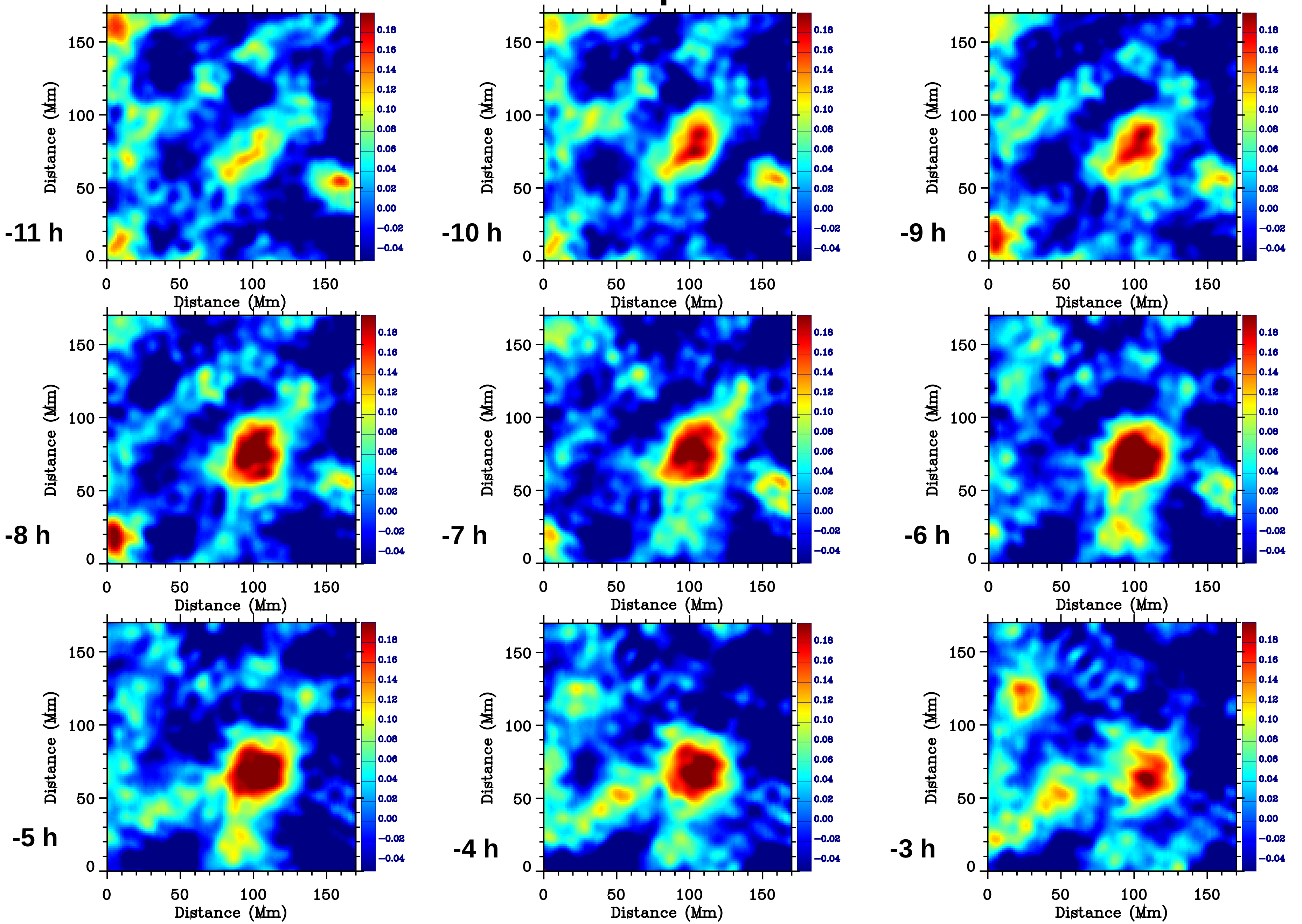

Results of AR 8164

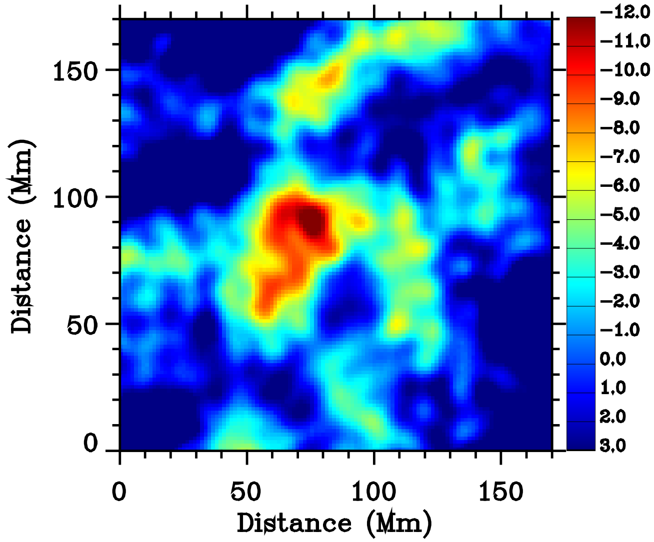

00:00 UT 23 Feb 1998

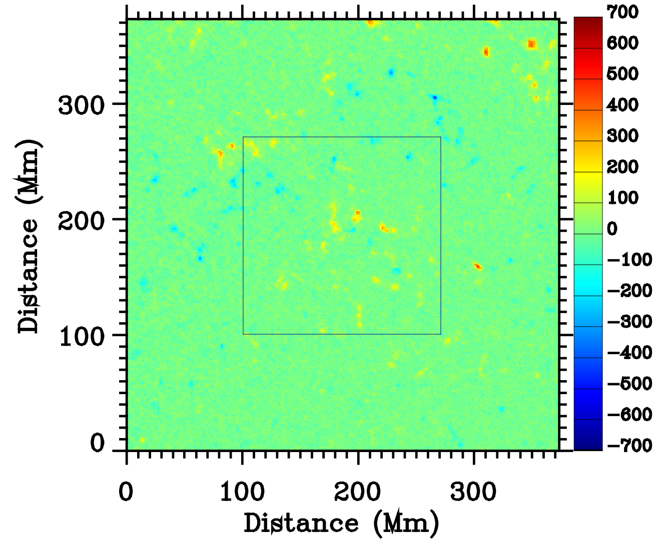

00:00 UT 23 Feb 1998

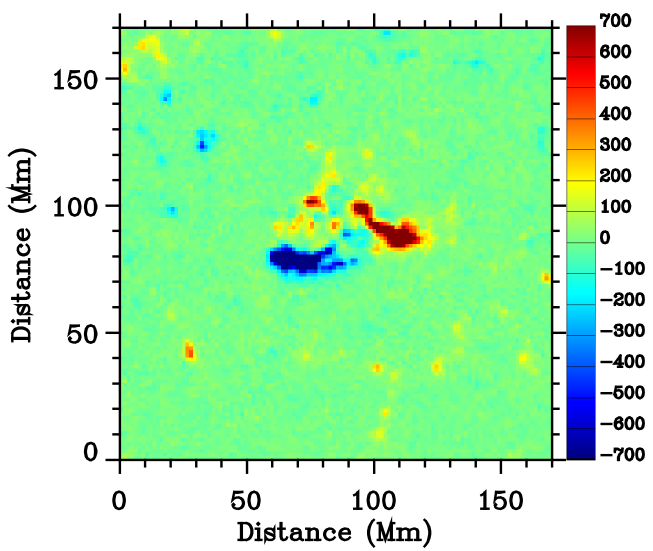

00:00 UT 24 Feb 1998

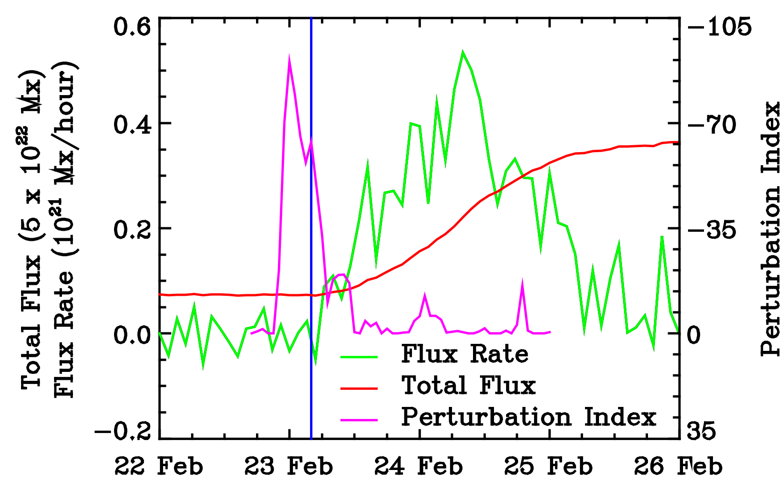

Results of AR 7978

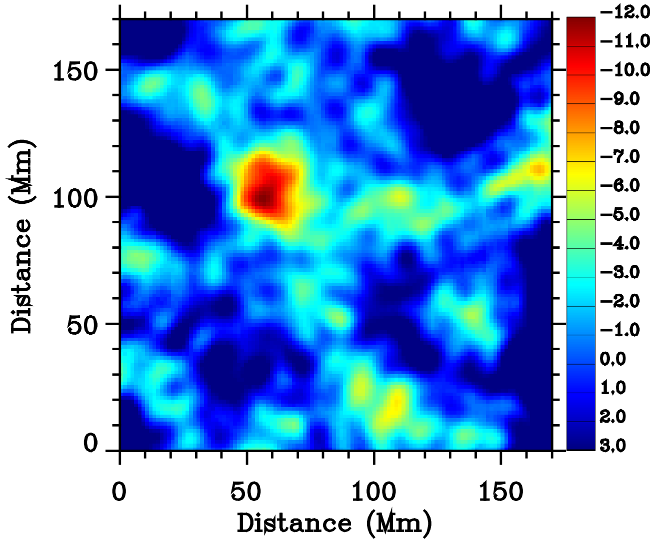

11:30 UT 06 Jul 1996

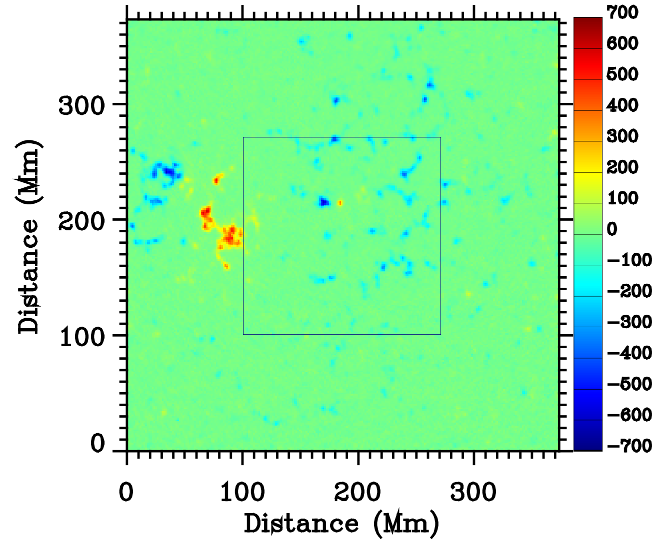

11:30 UT 06 Jul 1996

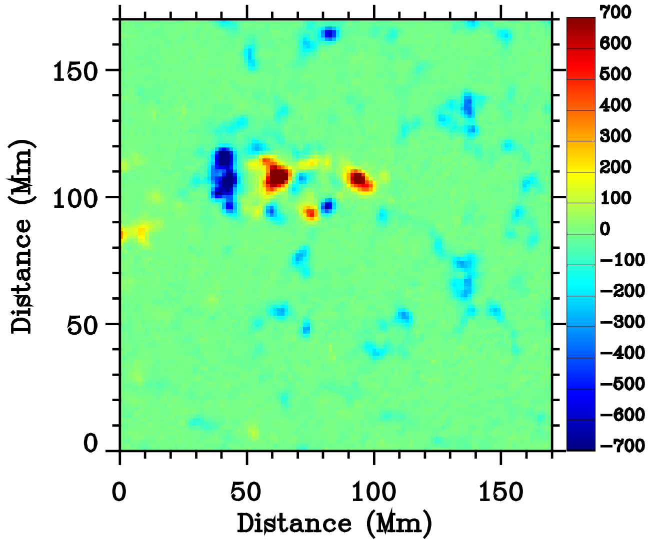

11:30 UT 07 Jul 1996

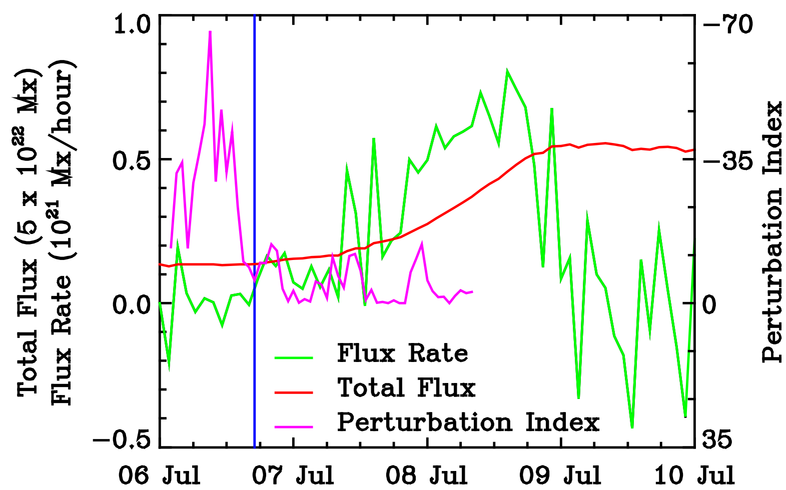

Results of AR 8171

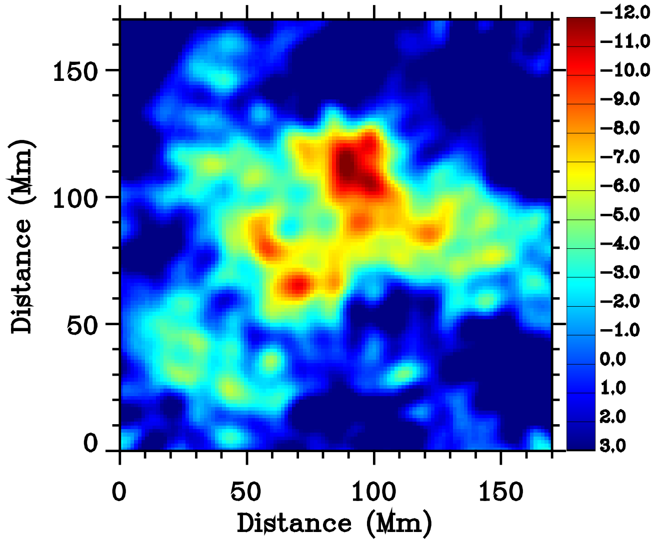

04:30 UT 27 Feb 1998

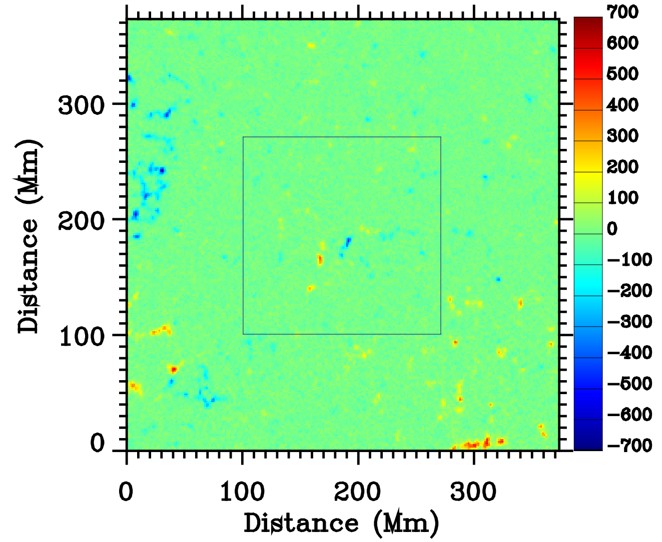

04:30 UT 27 Feb 1998

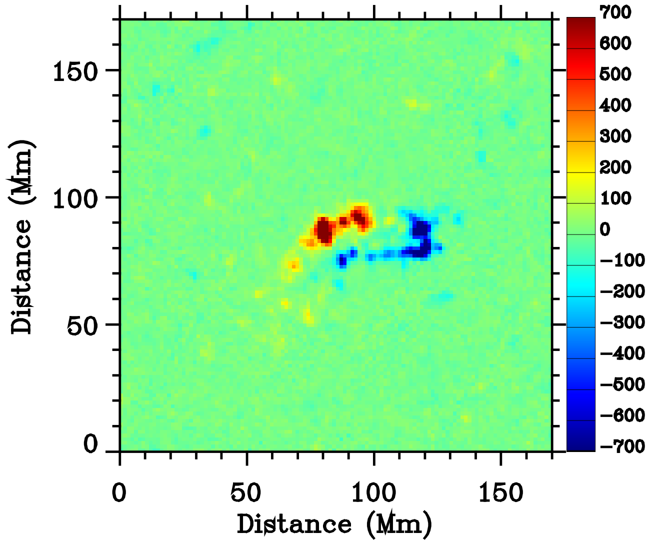

04:30 UT 28 Feb 1998

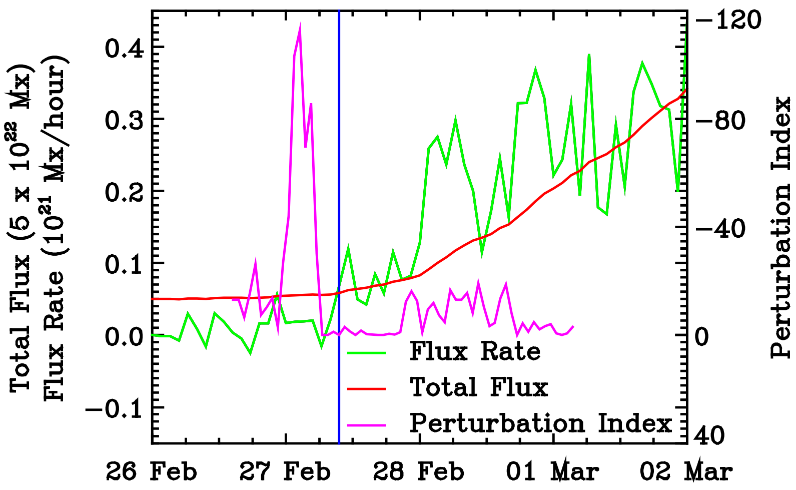

Estimates of noise level

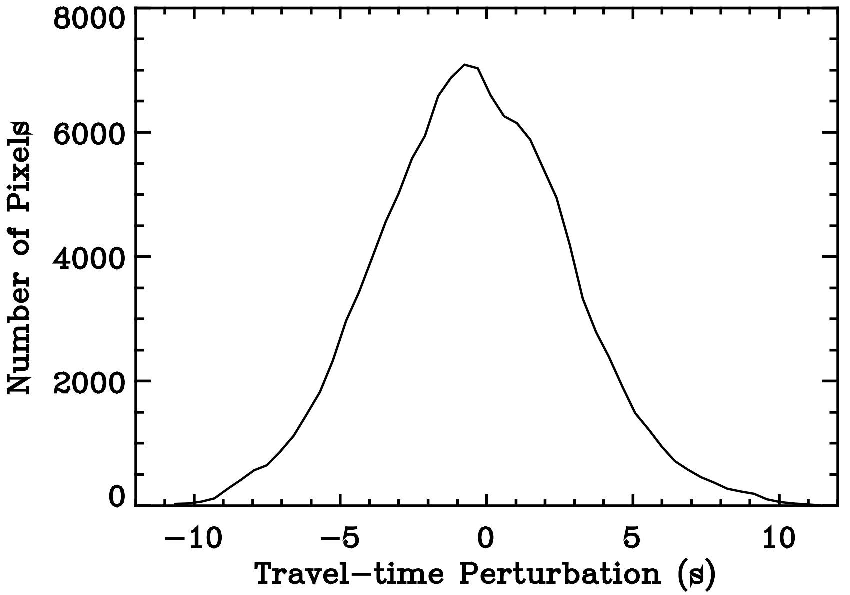

From 9 quiet regions:

1σ = 3.3 seconds

Active Region NOAA	Max travel-time perturbation (sec)	Signal-to-noise ratio
10488	16.3	4.9
8164	14.0	4.2
8171	12.5	3.8
7978	11.9	3.6

Results of AR 11158

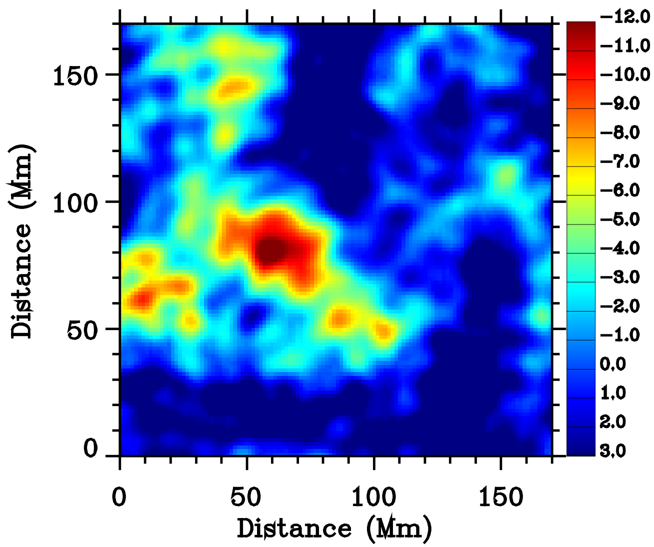

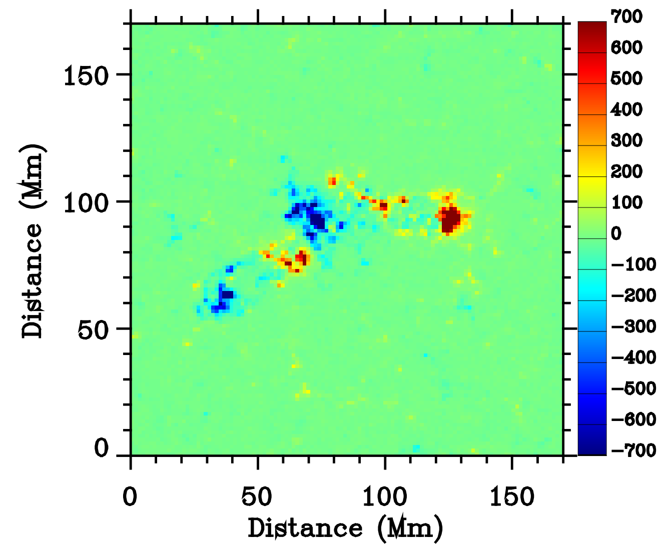

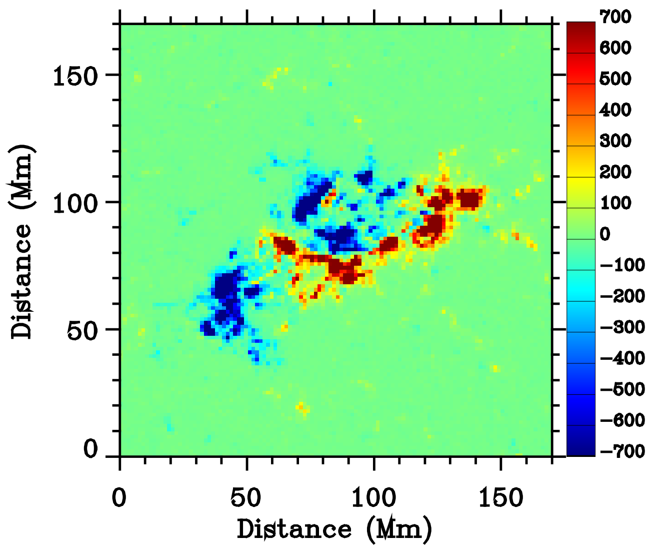

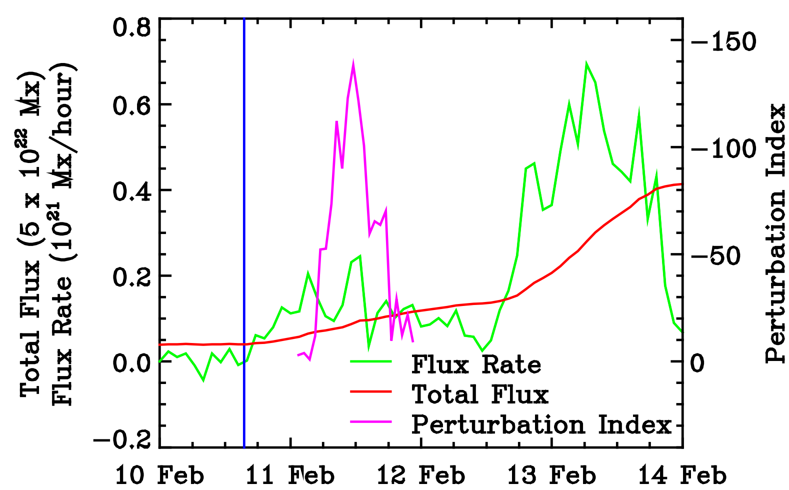

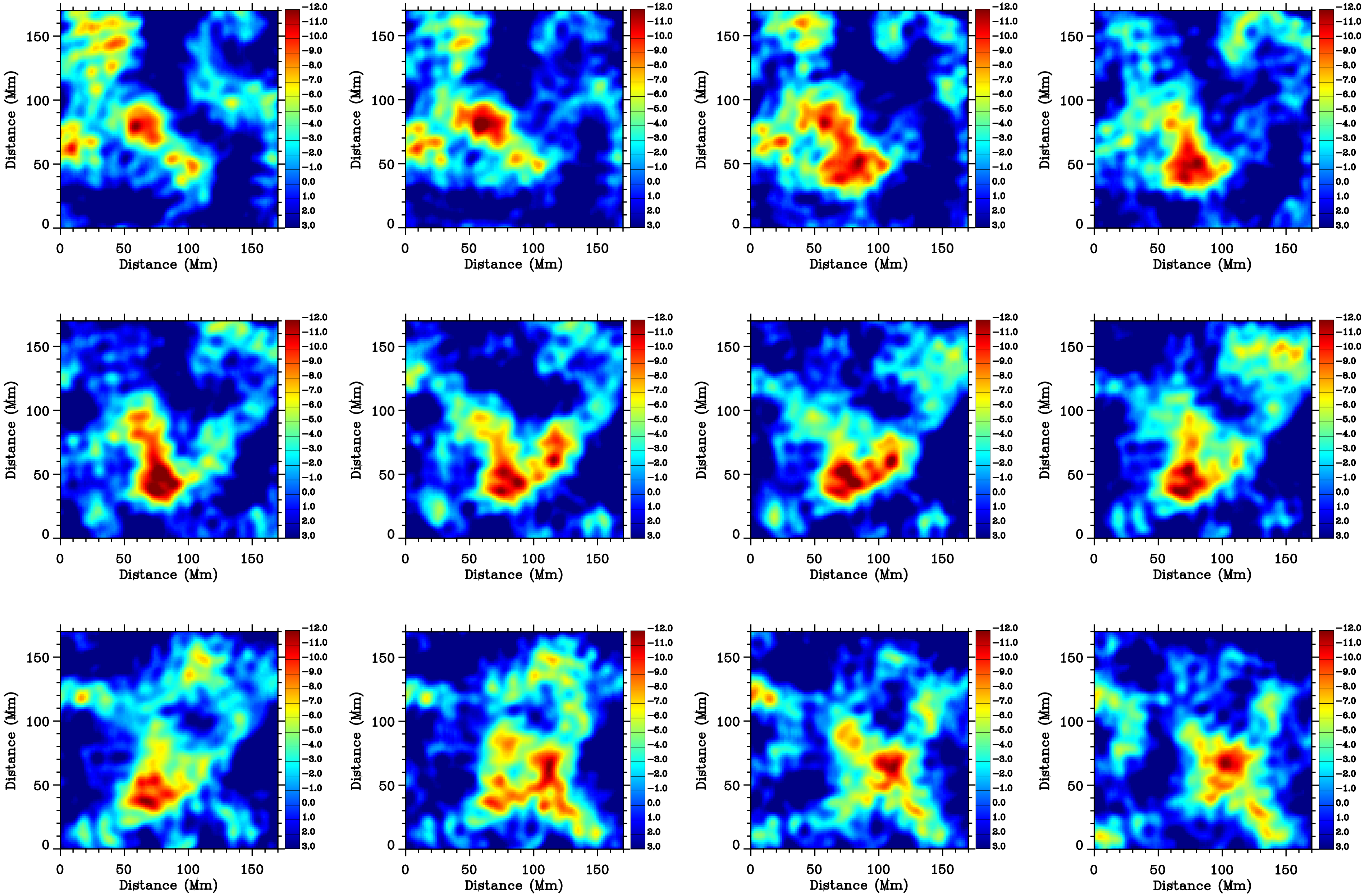

Distance (Mm)
Distance (Mm)
0
50
100
150
−12.0
−11.0
−10.0
−9.0
−8.0
−7.0
−6.0
−5.0
−4.0
−3.0
−2.0
−1.0
0.0
1.0
2.0
3.0

Comparison with Numerical Simulations

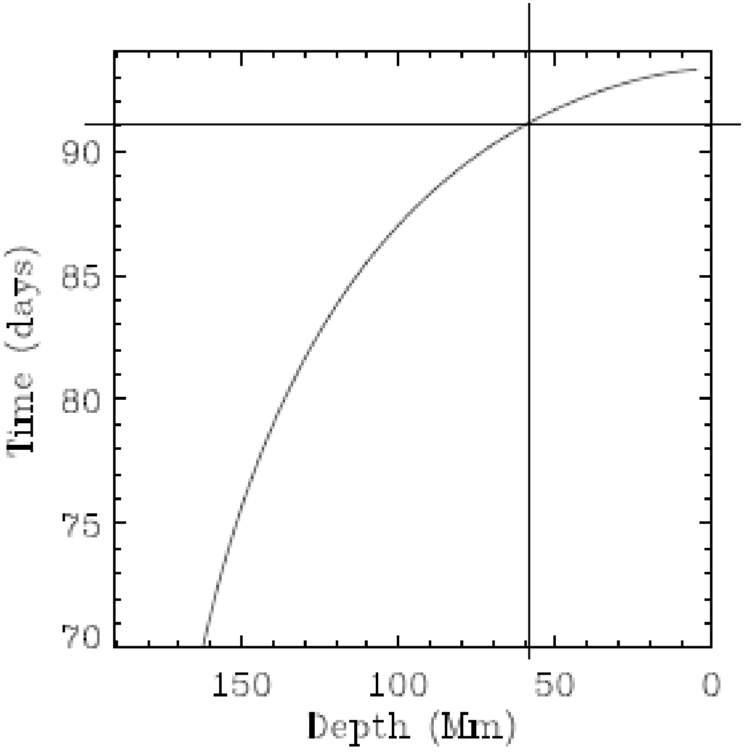

Thin flux tube simulation of an emerging Ω-shaped tube.

The figure shows the time since the onset of the Parker instability as a function of depth of the tube apex.

From: Yuhong Fan

Living Rev. Solar Phys., 6, (2009), 4

- Emerging time from a depth of 60 Mm until the surface = ~2 days.

  Consistent with our measurements of AR 7978.

- Rising flux tube models of Fan (2008) imply wave travel-time shifts of ~1 s (Birch et al., 2010).

  Inconsistent with our results (travel-time shifts of ~12-16 s).

Conclusions

1. Strong emerging flux events cause travel-time shifts of the order of 12-16 s at depths of 42-75 Mm and therefore they can be detected before the magnetic field emergence in the photosphere. It is not known what has caused these travel-time shifts.

2. The average emergence speed from a depth of ~60 Mm up to the surface is 0.6 and 0.3 km/s for the strongest and weakest analyzed events respectively. The detected anomalies appear at the surface 1-2 days after their detection. Therefore our method may improve space weather forecasts by allowing anticipation of large sunspot regions and predicting the development of an emerging flux region.

3. The detection of magnetic field at a depth of ~60 Mm possibly poses a low limit to the depth of generation of large magnetic active regions.

4. The amplitude of the detected travel-time shifts is at least 1 order of magnitude larger than the amplitude of the expected travel-time shifts based on numerical simulation models (with field strength 10^5 G at the bottom of the convection zone).

5. The detected structures at depths of 42-75 Mm are mostly circular with a typical size of 30-50 Mm. But the accuracy on the location and the shape of these structures is limited by the horizontal wavelength which is ~35 Mm at 3.5 mHz.